



1 Shear rate effect on the residual strength characteristics of saturated loess

2 Baoqin Lian^{a,b}, Jianbing Peng^{a*}, Qiangbing Huang^a

3

4 ^aCollege of Geological Engineering and Surveying, Chang'an University, Key

5 Laboratory of Western China Mineral Resources and Geological Engineering, Xi'an

6 710054, China

7

8 ^bDepartment of Geology & Geophysics, Texas A&M University, College Station, TX

9 77843-3115, United States

10

11 *Corresponding author: Jianbing Peng (dicexyl@gmail.com)

12

13

14


15

16



17 **Abstract**

18 Residual shear strength of soils is an important soil parameter for assessing the
19 stability of landslides. To investigate the effect of the shear rate on the residual shear
20 strength of loessic soils, a series of ring shear tests were carried out on loess from
21 three landslides at two shear rates (0.1 mm/min and 1 mm/min). Naturally drained
22 ring shear tests results showed that the shear displacement to achieve the residual
23 stage for specimens with higher shear rate was greater than that of the lower rate; both
24 the peak and residual friction coefficient became smaller with increase of shear rate
25 for each sample; at two shear rates, the residual friction coefficients for all specimens
26 under the lower normal stress were greater than that under the higher normal stress.

27 The tests results revealed that the difference in the residual friction angle ϕ_r at the two
28 shear rates, $\phi_r(1) - \phi_r(0.1)$, under each normal stress level were either positive or
29 negative values. However, the difference $\phi_r(1) - \phi_r(0.1)$ under all normal stresses
30 was negative, which indicates that the residual shear parameters reduced with the
31 increasing of the shear rate in loess area. Such negative shear rate effect on loess
32 could be attributed to a greater ability of clay particles in specimen to restore broken
33 bonds at low shear rates. 

34

35 **Keywords:** Loess; Residual shear strength; Ring shear test; Shear rate; Residual shear
36 parameter



37

38 **1. Introduction**



39 Residual shear strength of soil is of great significance for evaluating the stability
40 for the slip surface of first-time landslides as well as reactivated landslides (Bishop et
41 al., 1971; Mesri and Shahien, 2003). The residual strength of soils is defined as the
42 minimum constant value of strength along the slip plane, in which the soil particles
43 are reoriented and subjected to sufficiently large displacements in relatively low shear
44 rate (Skempton, 1985).

45 Numerical studies have been done to assess the residual strength through the
46 laboratory tests using ring shear tests and reversal direct shear tests (Moeyersons et al.,
47 2008; Summa et al., 2010; Vithana et al., 2012; Chen and Liu, 2013; Summa et al.,
48 2018). It is a generally accepted fact that the measurement of the residual strength is
49 most preferred done with a ring shear test since it allows the soil specimen be sheared
50 at unlimited displacement which can simulate the field conditions more accurately
51 (Lupini et al., 1981; Sassa et al., 2004; Tiwari and Marui, 2005; Bhat, 2013). Until
52 now, great efforts have been paid to the study of the shear rate effect on the minimum
53 value of clay or sand strength at residual states (Morgenstern and Hungr, 1984; Lemos,
54 1985; Tika, 1999; Tika and Hutchinson, 1999; Suzuki et al., 2007; Grelle and
55 Guadagno, 2010; Bhat, 2013). As a result, the residual strength of clay or sand under
56 the effect of shear rate has been made relatively clear. However, compared with the
57 results of tests on clay or sand, understanding of the shear characteristics of silty soil,
58 such as loess, is not yet complete. As pointed out by Ding (2016), some drained ring
59 shear tests have concluded that the increase in shear rate causes the residual strength



60 of loess to increase. On the contrary, Kimura et al. (2014) reported that the residual
61 strength of Malan loess decreases with the increase of shear rate. Furthermore, Wang
62 et al. (2015) found that the effect of shear rate on residual strength of loess is closely
63 associated with the normal stress levels, and the change in residual strength of loess
64 samples under high normal stress levels is small in ring shear tests.

65 Therefore, some inconsistent or even **opposite results** have been reported in the
66 ring shear tests on loess above, **which implied that there is still a lack of experimental**

67 **data on this top**  from the above investigations, it can be concluded that the effect of
68 the shear rate on the residual strength of the loess is not fully understood and needs
69 further scrutiny. Meanwhile, almost all of these investigations (Kimura et al., 2014;
70 Wang et al., 2015; Ding, 2016) focused on the residual shear characteristics of loess
71 obtained from the **same location**,  while studies of loess collected from different
72 locations have only been rarely performed. Moreover, it should be noted that the
73 residual strength parameters (friction angle) obtained from using different shear rates
74 may be adopted to provide a guide for designing some precision engineering which
75 require high accuracy of the design parameters, thus, the effect of the shear rate on the
76 residual strength of soils should be fully investigated to determine the parameters with
77 high reliability. In addition, residual strength parameters of soil play a key role in
78 assessing the stability analysis of landslides. Therefore, accurate determination of the
79 residual strength parameters and their dependence on the shear rate may affect the
80 stability evaluation of landslides. Thus, it is necessary to study the change of residual
81 strength of loess with shear rate in order to have a good understanding of the suitable



82 approach for the residual strength parameters measurement.

83 In this backdrop, to clarify the residual shear characteristics of loess under the
84 effect of the shear rate, a series of naturally drained ring shear tests were conducted on
85 loess obtained from three landslide sites at two shear rates (0.1 mm/min and 1 mm/min).
86 The residual shear characteristics of loess at the residual state was examined.
87 Considering that shear strength of loess reduces with moisture content (Dijkstra et al.,
88 1994; Zhang et al., 2009; Picarelli, 2010), ring shear tests were conducted on
89 saturated loess samples corresponding to the worst condition in field engineering.
90 Furthermore, this study investigated the change in the residual strength parameters of
91 loess at different shear rates and their relationships with the normal stress in naturally
92 drained ring shear tests as well.

93

94 **2. Geological setting of landslide sites**

95 Soil samples from three landslides in the northwest of China were selected in this
96 study. Soil samples used for the ring shear tests and index measuring tests
97 predominantly consist of loess deposits and were collected in a disturbed condition.
98 For convenience, the names of landslide sites were abbreviated into Djg, Ydg, and
99 Dbz. Fig. 1 shows the study sites and some views of the landslides.

100 **Dingjiagou landslide (Djg)**

101 The Djg landslide, located at the mouth of Dingjia Gully in Yan'an of China, is
102 geologically composed of upper loess and lower sand shale in the Yan-chang
103 formation. The dustpan-shaped landslide is inclined to the east, with its inclination
104 75.85°. The landslide is 350 m in width, 180 m in length, 70 m in elevation. The



105 average thickness of slip mass is around 20 m, and the volume of landslide totaled
106 approximately $105 \times 10^4 \text{ m}^3$. The slip mass is mainly constituted by loess, whereas the
107 sliding bed consists of sand shale in Yan-chang formation. The thickness of the
108 sliding zone varied from 30 to 50 cm. The front lateral region of the main slide
109 section of the Djg landslide, where the sampling was performed, was found to be silty
110 clay.


111 **Yandonggou landslide (Ydg)**

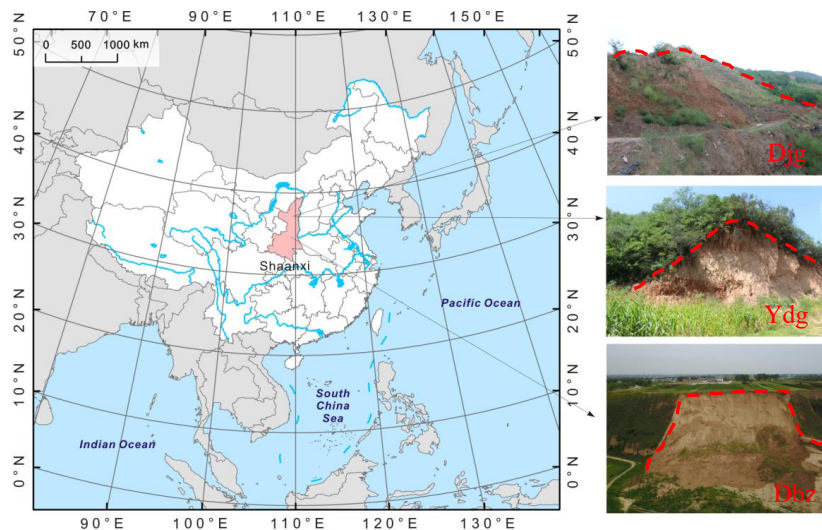
112 The Ydg landslide, located in the Qiaogou town of Yan'an in Shaan xi province of
113 China. The top and the toe altitude of the landslide are about 1165 m and 1110 m
114 above the sea level, with the height difference between the toe and the top of landslide
115 about 55 m. The slides have well-developed boundaries with the main sliding
116 direction of 240° and slope angle of 30° . From the landslides profile, the sliding
117 masses from top to bottom were classified by late Pleistocene (Q_3) loess, Lishi (Q_2)
118 loess and clay soil, respectively. Multiple landslides had occurred in this site, and the
119 soil samples used in this study were collected from Q_2 loess stratum within the slide
120 ranged from 4.5 m to 18 m in height.

121 **Dabuzi landslide (Dbz)**

122 The Dbz landslide located in the middle part of Shaanxi province (about E
123 $108^\circ 51' 36''$ and N $34^\circ 28' 48''$), China, which is a semi-arid zone dominated by loessic
124 geology. In this region, the investigated site is classified as a typical loess tableland
125 with quaternary stratum. The sedimentary losses in this area are grey yellow, and the
126 exposure stratum in this area has been divided into two stratigraphic units, namely,
127 the upper Malan (Q_3) loess and the lower Lishi (Q_2) loess, of which the Q_3 loess is



128 younger. The Q_3 loess is closest to the surface and is up to approximately 12 m thick,
129 while the thickness of Q_2 loess may reach an upper limit of about 50 m (Leng et al.,
130 2018). The loess in this area have well-developed vertical joints (Sun et al., 2009) 
131 The travel distance and the maximum width of the slip mass are roughly estimated to
132 be 122 m and 133 m, respectively. The armchair-shaped landslide shows an apparent
133 sliding plane, with an area of approximately 15,660 m² and about 66.25 m maximum
134 difference in elevation. The main direction of this landslide is approximately 355°.
135 The exposed side scarp of the landslide, where the sampling was done, was found to
136 be entirely in the Q_2 loess stratum.



137
138 Figure 1. Location of study sites and some views of landslides
139 Notes: Red dashed lines in the Figure 1 represent landslide boundary.

140 3. Experimental scheme

141 3.1. Testing sample

142 The fact that the residual shear strength is independent of the stress history has
143 been reported by many researchers (Bishop et al., 1971; Stark Timothy et al., 2005;



144 Vithana et al., 2012). Thus, disturbed loess samples from each landslide weighing
145 about 25 kg were collected to investigate the residual shear strength.

146 The soil samples were air-dried, and then crushed with a mortar and pestle. It was
147 found that small lumps may exist in air-dried samples, which may be too big for the
148 cell, so lumps were crushed in order to make sample uniform. This should be done
149 with care so as not to destroy silty-dominated loess. After that, soil samples were
150 processed through 0.5 mm sieve. Distilled water was then added to the soil samples
151 until saturated water content were obtained. The physical parameters such as natural
152 moisture content (*in-situ* moisture content), specific gravity, bulk density, plastic limit,
153 and liquid limit were determined in accordance with the Chinese National Standards
154 (CNS) GB/T 50123-1999 (standards for soil test methods) (SAC, 1999), but clay size
155 was defined to be less than 2 μm followed ASTM, D 422 (ASTM, 2007). Each soil
156 sample was separated into clay (sub 0.002 mm), silt (0.002-0.075 mm), and sand
157 (0.075-0.5 mm) fractions. The physical indexes of the soil are listed in Table 1.

158 The grain size distribution of soil was measured using a laser particle size
159 analyzer Bettersize 2000 (Dandong Bettersize Instruments Corporation, Dandong,
160 China). The sieved soil samples were used to determine particle size distribution



161 this study, soil samples were treated with sodium hexaphosphate, serving as a
162 dispersant, to disaggregate the bond between the particles. The results show that the
163 clay fraction in Djg landslide soil (24%) is more than two times than that from Ydg
164 (9%) and Dbz (9.1%). Furthermore, the particle size analysis illustrated that the
165 percentage of silt-sized soil in three landslides ranged from 75.66% to 87.4%. In



166 addition, Ydg landslide soil consists of the greatest percentage of the sand fraction
 167 which reaches up to 10.55%.

168 **Table 1** Physical parameters of slip-zone loess

| sites | ρ_d | W | ρ | G_s | W_L | W_p | Grain size fractions (%) | | | |
|-------|----------|------|--------|-------|-------|-------|--------------------------|---------------|-------------|-------------|
| | | | | | | | <0.002mm | 0.002-0.005mm | 0.005-0.075 | 0.075-0.5mm |
| Djg | 1.74 | 19.5 | 2.08 | 2.65 | 36 | 20 | 24 | 11.48 | 64.18 | 0.34 |
| Ydg | 1.47 | 18 | 1.74 | 2.71 | 33 | 19 | 9 | 5.28 | 75.17 | 10.55 |
| Dbz | 1.48 | 16 | 1.72 | 2.70 | 32 | 21 | 9.1 | 6.4 | 81 | 3.5 |

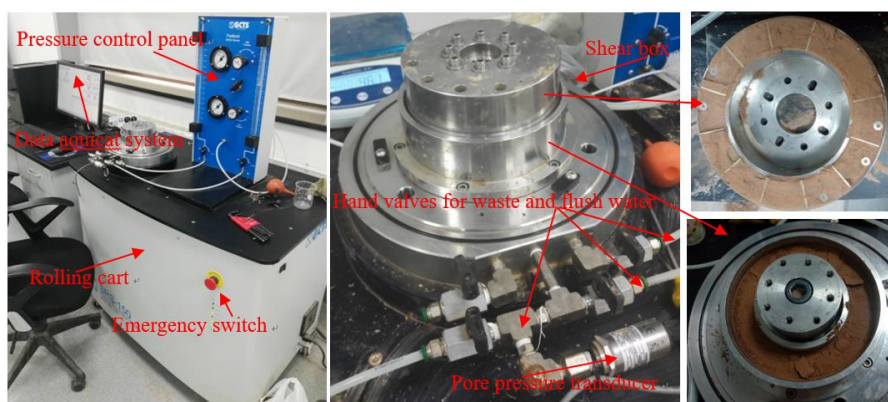
169 Notes: ρ_d = dry density (g/cm^3); w =moisture water content (%); ρ = bulk density
 170 (g/cm^3); G_s = specific gravity; W_L =liquid limit; W_p = plastic limit

171 **3.2. Testing apparatus**

172 An advanced ring shearing apparatus (SRS-150) manufactured by GCTS (Arizona,
 173 USA) was adopted in ring shear tests and the photos of apparatus were shown in Fig.
 174 2, which consists mainly of a shear box with an outer diameter of 150 mm, an inter
 175 diameter of 100 mm and the maximal sample height of 250 mm. The shearing box
 176 consists of the upper shear box and the lower shear box. In the shearing process, the
 177 upper shear box keeps still while the lower one rotates. The apparatus which provides
 178 effective specimen area of 98 cm^2 , is capable of shearing the specimen for large
 179 displacements. The annular specimen is confined by inside and outside metal rings.
 180 Moreover, the specimen is confined by bottom annular porous plates and top annular
 181 porous plates in which have sharp-edged radial metal fins which protrude vertically
 182 into the top and bottom of the specimen at the shearing process. Two annual porous
 183 plates were used to provide drainage condition in the test following previous research
 184 (Stark and Vettel, 1992). The normal stress, shear strength and shear displacement can



185 be monitored by computer in shearing process. The measurement features of the ring
186 shear apparatus employed in this study are described as follows: shear rate range from
187 0.001 degrees to 360 degrees per minute, 10 kN axial load capacity, 300 N
188 continuous torque capacity, maximum normal stress of 1000 kN/m².



189
190 Figure 2. Ring shear apparatus (SRS-150)

191 3.3. Testing procedure



192 In present study, reconstituted samples of the sub 0.5 mm soil fractions were used
193 in the testing as it was reported that the residual strength of the soil was unaffected by
194 its initial structure (Gibson et al., 1971; Vithana et al., 2012). Specimens were first
195 prepared by adding distilled water to the air-dried soil until the saturated moisture
196 contents were obtained. Then, specimens were kept in a sealed container for at least
197 one week to fully hydrate. Afterwards, specimens are reconstituted in the ring-shaped
198 chamber of the apparatus by compaction. The specimen was then consolidated under
199 a specific effective normal stress in a range of 100 kN/m² to 400 kN/m² until
200 consolidation was achieved. In this study, consolidation was completed when the
201 consolidation deformation was smaller than 0.01 mm within 24 hr (Kramer et al.,
202 1999; Shinohara and Golman, 2002). Then, the consolidated specimen is subjected to



203 shearing under constant normal stress by rotating the lower half of the shear box
204 attached to a gear, while the upper half remains still. In ring shear tests, the normal
205 stress at the shearing was the same as at consolidation stage. Shear strength of loess
206 specimen was recorded at intervals of 1s before the peak shear strength, after the peak,
207 the sampling rate was increased to 1 min.

208 In this study, ring shear tests were performed in a single stage under naturally
209 drained condition and the samples were subjected to shear until the residual state was
210 achieved. Drained condition of the shearing process is provided by two porous stones
211 attached on the top and the bottom platen of the specimen container. As for soil
212 specimens with low permeability, the rate of excess pore pressure generation in the
213 shear box may exceeded that of pore-pressure dissipation, this type of condition is
214 identified as naturally drained condition in previous studies (Linda et al., 2004).
215 Furthermore, Tiwari (2000) asserted that it was acceptable to use a shear rate below
216 1.1 mm/min to simulate the field naturally drained condition. Thus, shear rates of 0.1
217 mm/min and 1 mm/min were used in this study to simulate the naturally drained
218 condition of the slip zone soils.

219 4. Results

220 Twenty -four specimens were tested to investigate the residual shear
221 characteristics of the saturated loess in the ring shear apparatus. Residual shear
222 strength of loess was determined following the research conducted by Bromhead
223 (1992) who pointed out that the residual stage is attained if a constant shear stress is
224 measured for more than half an hour. Tests results are shown in this section.



225 **4.1. Shear behavior**

226 Figs. 3(a)- 5(a) show the typical shear characteristics of the loess (shear rate of 0.1
227 mm/min and 1 mm/min) obtained from three different locations, where, the shear
228 stress is plotted against the shear displacement. It is a widely accepted fact that
229 normal stress has effect on the shear behavior of the soil (Stark Timothy et al., 2005;
230 Eid, 2014; Kimura et al., 2015; Wang et al., 2019), thus, the shear behavior of
231 samples at the peak and residual stages, where, the determined peak friction
232 coefficient as well as residual friction coefficient are plotted in Figs. 3(b)-5(b) against
233 the corresponding effective normal stresses as well. The friction coefficient is defined
234 as the shear stress divided by the effective normal stress.

235 Figs. 3(a)-5(a) demonstrate that shear stress increases dramatically within small
236 shear displacement and then reduces with shear displacement, until residual
237 conditions were achieved at large displacements. Furthermore, it is obvious that the
238 peak strength and the residual strength of samples with high shear rate are almost
239 smaller than that of the samples with low shear rate. It can be found that shear
240 displacement to achieve the residual stage for specimens with high shear rate is
241 greater than that of the low rate. For example, the minimum shear displacements for
242 attaining residual condition for Djg specimens with low and high shear rate were
243 about 360 mm and 650 mm, respectively. Under the shear rate of 0.1 mm/min and 1
244 mm/min, Ydg specimens need approximately 80 mm and 1,400 mm displacement to
245 achieve residual stage. However, Dbz specimens require about 40 mm and 60 mm
246 displacement to reach residual condition for low and high shear rate, respectively.



247 In Figs. 3(a)- 5(a), a clear drop can be seen, at any normal stress, for specimens
248 obtained from all sites. It is obvious that Djg specimens showed greater peak-post
249 drop than that of Ydg and Dbz specimens. For example, at the normal stress of 100
250 kN/m², Djg samples show approximately 47.3% and 36.8% decrease from the peak
251 friction coefficient to the residual friction coefficient at low and high shear rates (Fig.
252 3(b)), respectively, which is greater than in the Ydg samples (about 9.8% and 10.3%
253 in Fig. 4(b)) and Dbz samples (about 2.4% and 3.2% in Fig. 5(b)). In Djg samples, an
254 obvious slickenside was observed on the shear surface (Fig. 6). This phenomenon
255 indicates a high degree of reorientation of platy clay minerals parallel to the direction
256 of shearing. In Figs. 3(b)- 5(b), on average, it was found that the decrease in the
257 friction coefficient from the peak strength in the Djg sample is almost 18.1% and
258 21.3% for the sample consolidated at normal stress of 400 kN/m² under the low and
259 high shear rate (Fig. 3(b)), while such reduction in friction coefficient in Ydg sample
260 are only about 4.1% and 4.8% (Fig. 4(b)). Furthermore, under the low and high shear
261 rate, the friction coefficient reduction in Dbz samples are only approximately 5.6%
262 and 6.0% (Fig. 5(b)). Skempton (1985) reported that the strength of soils falls to the
263 residual value in ring shear tests, owing to reorientation of platy clay minerals parallel
264 to the direction of shearing. Based on the conclusion that the post-peak drop in
265 strength of normally consolidated soil is only due to particle reorientation after the
266 peak strength (Skempton, 1964; Mesri and Shahien, 2003), the results demonstrated
267 that the Djg landslide soil existed the greater particle reorientation compared with that
268 of other two landslide soils.



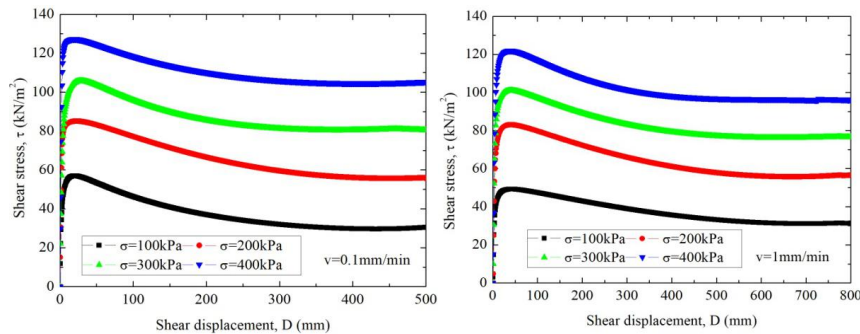


269

270 **4.2. Effect of normal stress on the friction coefficients**

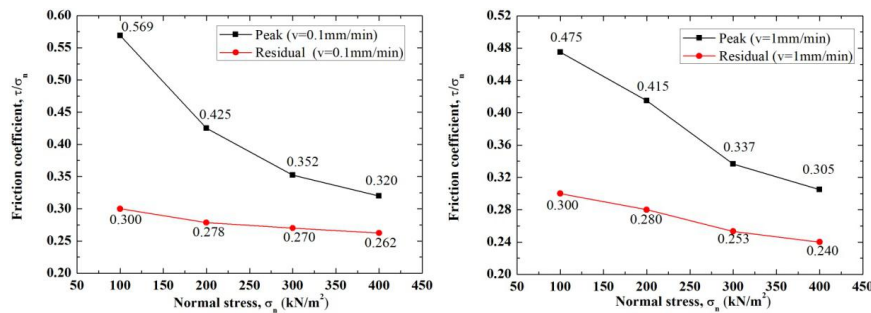


271 It can be seen from the Figs. 3(b)-5(b) that the friction coefficients (peak and
 272 residual) are higher at low effective normal stress levels compared with that at high
 273 normal stress. For example, with normal stress increasing from 100 kN/m² to 400
 274 kN/m², the peak and residual friction coefficient of Djg landslide soils at the shear
 275 rate of 0.1 mm/min reduce from 0.569 to 0.32 and from 0.3 to 0.262 (Fig. 3(b)),
 276 respectively. Similarly, results obtained from other two landslides loess also show that
 277 the friction coefficients decrease nonlinearly with normal stresses (Figs. 4(b) and
 278 5(b)). Furthermore, specimens with shear rate of 0.1 mm/min attained greater friction
 279 coefficients than that with shear rate of 1 mm/min (Figs. 3(b)-5(b)).



280

281 (a) Relationship between shear stress and shear displacement



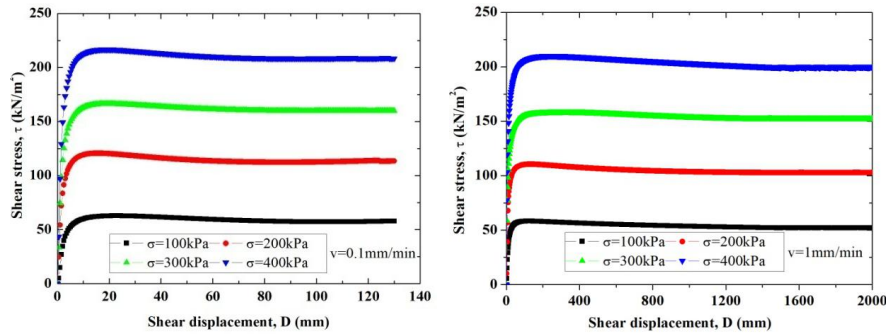
282

283 (b) Relationship between friction coefficient and normal stress



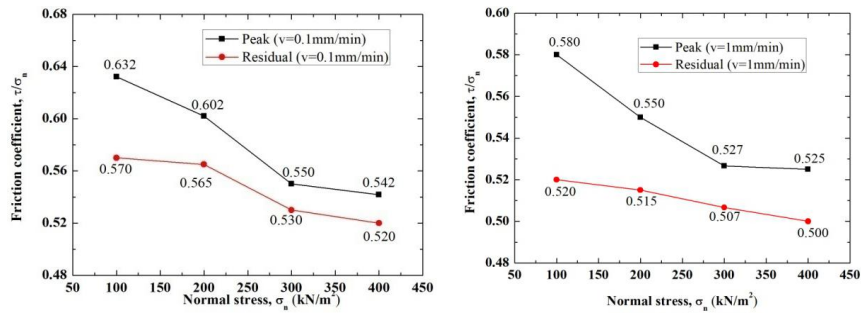
284 Figure 3. Shear behavior characteristics of Djg soil samples

285



286

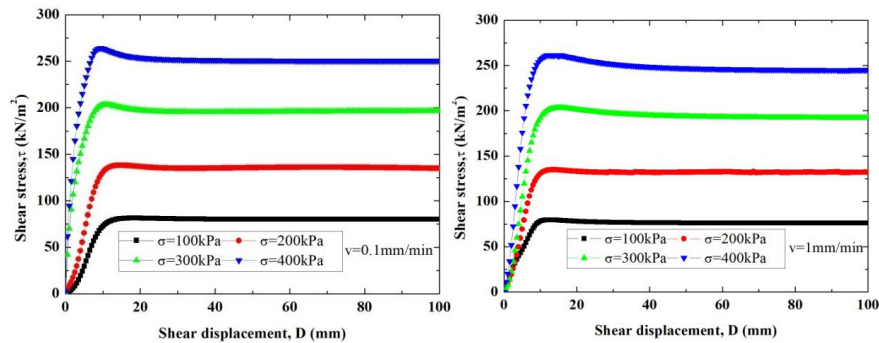
287 (a) Relationship between shear stress and shear displacement



288

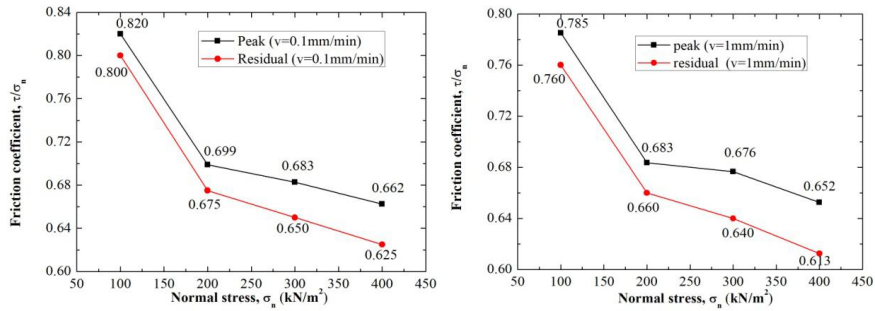
289 (b) Relationship between friction coefficient and normal stress

290 Figure 4. Shear behavior characteristics of Ydg soil samples



291

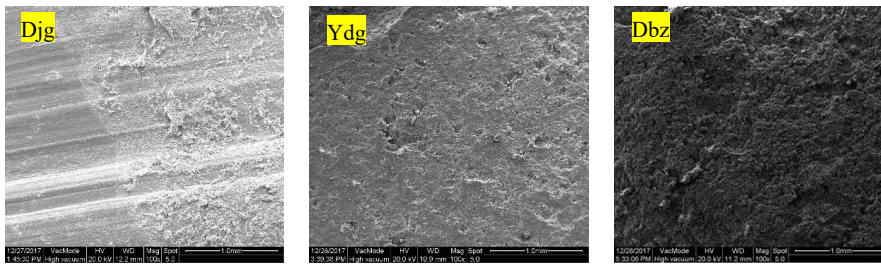
292 (a) Relationship between shear stress and shear displacement



293

294 (b) Relationship between friction coefficient and normal stress

295 Figure 5. Shear behavior characteristics of the Dbz soil samples



296

297 Figure 6. SEM photographs of the shear surface of loess samples (100 magnification)

298 4.3. Effects of shear rate on residual strength parameter



299 For the samples described above, Figs. 7-9 show the relationships between the

300 residual friction coefficient and the normal stress, and the residual strength parameters.

301 The residual friction coefficient is plotted against the normal stress. The residual

302 friction coefficient is defined as the residual shear strength divided by normal stress. It

303 has been recognized that the shear strength parameters including cohesion and friction

304 angle (Terzaghi, 1951; Stark Timothy et al., 2005). However, according to the

305 previous studies, the residual angle of soils varies depended on the soil properties as

306 well as the magnitude of normal stress provided the residual cohesion of soil is zero

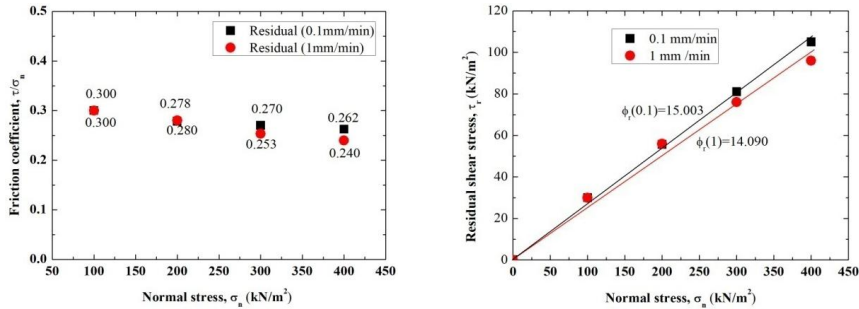
307 (Skempton, 1964; Bishop; Kimura et al., 2014). Thus, in this study, the residual

308 frictions are calculated by Coulomb's law assumed the residual cohesion is zero



309 following the previous studies (Skempton, 1985). The residual strength parameters
310 were defined as $\phi_r(0.1)$ and $\phi_r(1)$ at the low shear rate and high shear rate,
311 respectively. And the difference between the residual friction angles at two shear rates
312 was defined as $\phi_r(1) - \phi_r(0.1)$. Comparatively, the residual friction coefficient was
313 defined as $\tau_r/\sigma_n(0.1)$ at the low shear rate and $\tau_r/\sigma_n(1)$ at the high shear rate,
314 respectively. Furthermore, the difference between the residual friction coefficients
315 was defined as $\tau_r/\sigma_n(1) - \tau_r/\sigma_n(0.1)$. Table 2 summarized the residual shear
316 parameters of the landslide soils.

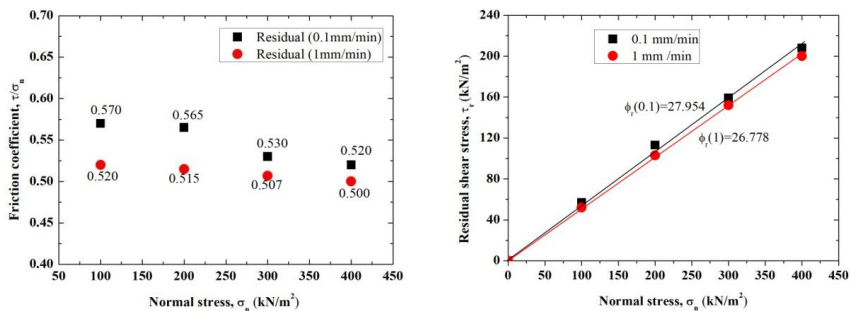
317 Fig. 7 shows that the residual friction coefficients are relatively low in Djg
318 samples. The coefficients $\tau_r/\sigma_n(0.1)$ and $\tau_r/\sigma_n(1)$ at the normal stress of 100 kN/m²
319 to 400 kN/m² ranged from 0.3 to 0.262 and from 0.3 to 0.24, respectively. The
320 difference between the friction coefficients, $\tau_r/\sigma_n(1) - \tau_r/\sigma_n(0.1)$, at each normal
321 stress level are varied in a range of -0.022 to +0.002. For the difference between the
322 residual friction angles, $\phi_r(1) - \phi_r(0.1)$, ranged from -1.212° to +0.079° (Table 2). For
323 normal stress above 200 kN/m², the residual friction coefficient $\tau_r/\sigma_n(0.1)$ was found
324 to be greater than the residual friction coefficient $\tau_r/\sigma_n(1)$. For this sample, residual
325 friction coefficients show a slight decrease with the shear rate for normal stress above
326 200 kN/m².



327

328 Figure 7. Relationships between residual shear stress and normal stress, and
 329 residual strength parameter for Djg soil sample

330 Fig. 8 gives the results of the Ydg samples. The coefficients $\tau_r/\sigma_n(0.1)$ and τ_r/σ_n
 331 (1) under the normal stress of 100 kN/m² to 400 kN/m² ranged from 0.57 to 0.52 and
 332 from 0.52 to 0.50, respectively. Furthermore, the difference $\tau_r/\sigma_n(1) - \tau_r/\sigma_n(0.1)$ at
 333 each normal stress was from -0.05 to -0.02. As for the difference between the residual
 334 friction angles, $\phi_r(1) - \phi_r(0.1)$, was in a range of -2.218° to -0.909°. In case of Ydg
 335 soil sample, the residual friction coefficients decreased with increase of shear rate for
 336 all normal stress levels.



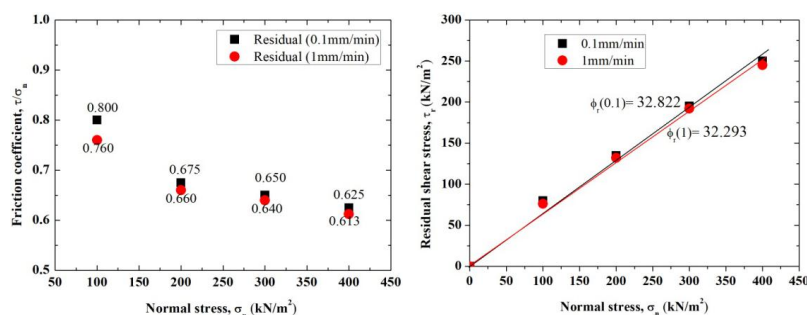
337

338 Figure 8. Relationships between residual shear stress and normal stress, and residual
 339 strength parameter for Ydg soil samples

340 Fig. 9 presents the results of the Dbz samples. The coefficients $\tau_r/\sigma_n(0.1)$ and τ_r/σ_n
 341 (1) at the normal stress of 100 kN/m² to 400 kN/m² ranged from 0.8 to 0.625 and



342 from 0.76 to 0.613, respectively. The difference $\tau_r/\sigma_n(1) - \tau_r/\sigma_n(0.1)$ at each normal
 343 stress was from -0.04 to -0.01. The difference $\phi_r(1) - \phi_r(0.1)$ was from -1.425° to
 344 -0.405° . For Dbz samples, there was somewhat decrease tendency of the residual
 345 friction coefficients with the increasing of the shear rate for all normal stress levels. It
 346 is noted that the maximum difference was found at the lowest normal stress of 100
 347 kN/m^2 .



348
 349 Figure 9. Relationships between residual shear stress and normal stress, and residual
 350 strength parameter for Dbz soil sample

351 Table 2 summarizes residual strength parameters including $\phi_r(0.1)$ and $\phi_r(1)$ of
 352 all specimens obtained from the ring shear tests in this study. As for the Djg samples,
 353 the residual strength parameter $\phi_r(0.1)$ and $\phi_r(1)$ for all normal stress were found to
 354 be 15.003° and 14.09° (Fig. 7), respectively. However, the residual friction angles ϕ_r
 355 (0.1) and $\phi_r(1)$ of the Ydg samples were obtained to be 27.954° and 26.778° (Fig. 8),
 356 respectively. In the case of Dbz sample, the friction angles $\phi_r(0.1)$ and $\phi_r(1)$ were
 357 high, 32.822° and 32.293° (Fig. 9), respectively. The residual friction angles $\phi_r(0.1)$
 358 and $\phi_r(1)$ under all normal stresses were from 15.003° to 32.822° and from 14.09° to
 359 32.293° , respectively.

360 Due to the influence of the shear rate, the difference $\phi_r(1) - \phi_r(0.1)$ in the Djg,



361 Ydg and Dbz samples, were -0.913° , -1.176° and -0.529° , respectively. Wang (2014)
 362 and Fan et al. (2017) asserted that the residual shear strength of remolded loess hardly
 363 affected by shear rate below 5 mm/min. However, the results in this study shown that
 364 $\phi_r(1) - \phi_r(0.1)$ under all normal stress levels were negative for loess. Moreover, the
 365 absolute value of $\phi_r(1) - \phi_r(0.1)$ in Ydg samples even reached up to 1.176° .

366

367 Table 2 Residual shear strength parameter of landslide soils

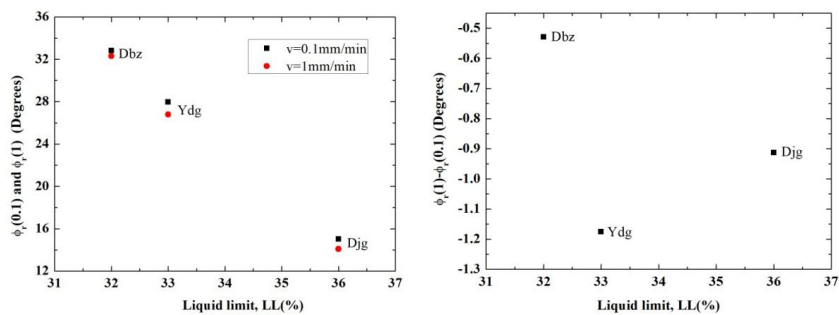
| No | Sample | Normal stress(kN/m ²) | Residual strength parameter | | | | Difference in parameter | |
|----|--------|-----------------------------------|---|-----------------------|-------------------------------------|-----------------------|-------------------------------------|--------|
| | | | 0.1 mm/min $\phi_r(0.1)$ ($c_r(0.1)=0$) | | 1 mm/min $\phi_r(1)$ ($c_r(1)=0$) | | $\phi_r(1) - \phi_r(0.1)$ (Degrees) | |
| | | | (Degrees) | | (Degrees) | | | |
| | | Under each σ_n | Under all σ_n | Under each σ_n | Under all σ_n | Under each σ_n | Under all σ_n | |
| 1 | Djg | 100 | 16.699 | 15.003 | 16.699 | 14.090 | 0 | -0.913 |
| | | 200 | 15.563 | | 15.642 | | 0.079 | |
| | | 300 | 15.110 | | 14.216 | | -0.894 | |
| | | 400 | 14.708 | | 13.496 | | -1.212 | |
| 2 | Ydg | 100 | 29.683 | 27.954 | 27.474 | 26.778 | -2.209 | -1.176 |
| | | 200 | 29.466 | | 27.248 | | -2.218 | |
| | | 300 | 27.923 | | 26.870 | | -1.053 | |
| | | 400 | 27.474 | | 26.565 | | -0.909 | |
| 3 | Dbz | 100 | 38.660 | 32.822 | 37.235 | 32.293 | -1.425 | -0.529 |
| | | 200 | 34.019 | | 33.425 | | -0.594 | |
| | | 300 | 33.024 | | 32.619 | | -0.405 | |
| | | 400 | 32.005 | | 31.487 | | -0.518 | |

368

369 **4.4. Influence of the shear rate on the residual friction angles according to soil**
 370 **properties**



371 It has been recognized that residual shear strength of soils is closely related with
372 soil properties, such as particle size distribution (PSD), liquid limit (LL), plasticity
373 index (I_p) and clay fraction (CF) (Terzaghi et al., 1996). Fig. 10 depicts the
374 relationships between residual friction angles as well as the difference in the residual
375 friction angles and soil properties including liquid limit (LL), plasticity index (I_p) and
376 clay fraction (CF) at two shear rates. The residual friction angles at two shear rates
377 decreased nonlinearly with the increasing of the LL. As for the relationship between
378 the ϕ_r and I_p , the ϕ_r under the low and high shear rates decreases from about 32° to 15°
379 with increasing the I_p from 11 to 16. These findings agree well with the early studies
380 (Wesley, 2003; Tiwari et al., 2005). With increasing of CF from 9% to 24%, the
381 residual friction angles under low and high shear rates were found to decrease (Fig.
382 10). These observations are consistent with previous studies (Lupini et al., 1981; Gibo
383 et al., 1987). Interestingly, for Dbz and Ydg soils of which have similar percentage of
384 clay fraction, the residual friction angles at both shear rates varied. However, in the
385 relationships between the difference in the residual friction angles and the soil
386 properties, no clear correlations were found.



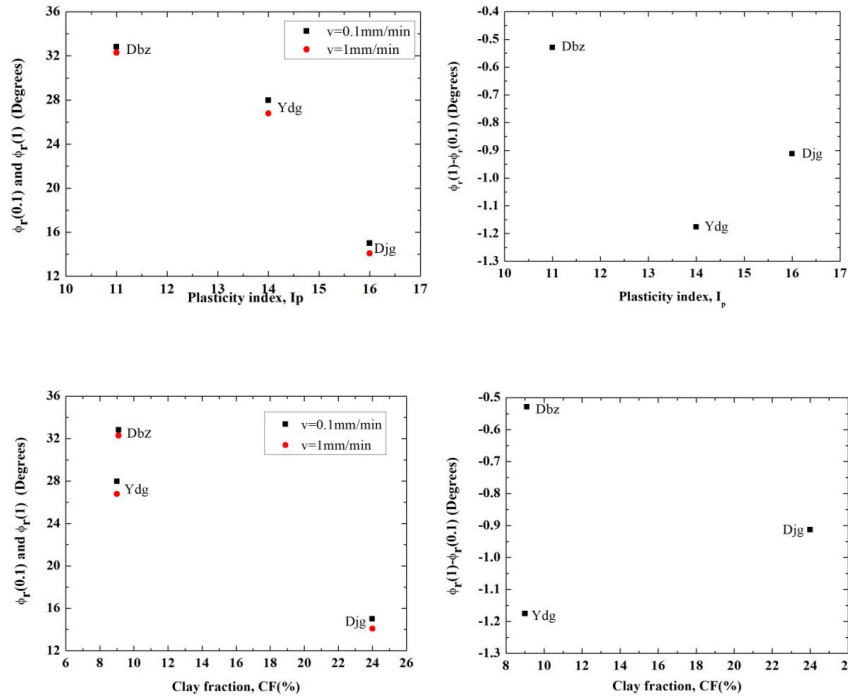
387

388



389

390



391

392 Figure 10. Relationships between residual shear parameter, the difference in
393 residual shear parameter and the soil properties at two shear rates

394 5. Discussion

395 Examination of the ring shear test results provides a basis for some general
396 comments on the use of tests results with different shear rates, partially deepening
397 some aspects deriving from previous studies.

398 From the experimental results on the three selected landslides, it was found that
399 there is a negative relationship between residual friction coefficients and shear rates
400 for all samples (Figs. 7, 8 and 9). Such a negative effect of shear rate (higher residual
401 friction coefficients at lower rates) has been reported in the literature for fine-grained
402 soils (Tika et al., 1996; Gratchev Ivan and Sassa, 2015). This effect may be closely
403 associated with ability of clay particles in specimen to restore broken bonds at



404 different shear rates. Previous studies (Osipov et al., 1984; Perret et al., 1996).
405 concluded that with higher shear rates, the breakdown of the bonds between clay
406 particles or flocs exceeds the restoration bond, leading to reduction in residual friction
407 coefficients. In contrast, the bonds between particles are rebuilt quickly and the
408 recovery rate can catch up the breakdown rate at lower shear rates. Therefore, the
409 weaker bonding between particles could explain the strength drop with the increasing
410 of the shear rate in this study.

411 The difference between the friction coefficients, $\tau_r/\sigma_n(1) - \tau_r/\sigma_n(0.1)$, at each
412 normal stress level varies in different locations. $\tau_r/\sigma_n(1) - \tau_r/\sigma_n(0.1)$ in Ydg specimen
413 are greater compared with that in Djg and in Dbz specimen (Table 2). As for Ydg and
414 Dbz specimen, it is found that the shear rate effect on the friction coefficient can be
415 seen to decrease with normal stress (Figs. 8 and 9). By contrast, there is an increasing
416 tendency in the influence of shear rate on the friction coefficient with normal stress in
417 Djg specimen (Fig. 7). Gibo et al. (1987) reported that the residual friction angle of
418 soils was controlled by the effective normal stress as well as by the CF. Interestingly,
419 Ydg (with CF 9%) and Dbz (with CF 9.1%) specimens with almost the same fraction
420 of clay showed similar shear rate effect on the residual friction coefficient with
421 normal stress increasing, however, Djg (with 24% CF) showed the contrast tendency
422 of shear rate effect on residual friction coefficient with normal stress, indicating that
423 such effect is closely associated with CF. Therefore, as for Ydg and Dbz with
424 relatively low fraction of CF, there is an increase effect of shear rate on residual
425 friction coefficient with decreasing of normal stress. Thus, for the application of



426 measured residual friction coefficient for stability analysis of shallow landslides with
427 lower overburden pressure, it is significant for us to use a low shear rate in ring shear
428 tests to measure residual shear strength parameters. On other hand, for Djg with high
429 CF, it is more reliable to use a low shear rate in ring shear tests to determine residual
430 friction coefficient for stability analysis of deep landslides with high overburden
431 pressure.

432

433 **6. Conclusion**

434 A series of ring shear tests were conducted on loess obtained from three landslides
435 to study the residual shear characteristics of saturated loess. Based on the test results,
436 the effect of the shear rate on the residual shear characteristics of loess in naturally
437 drained condition was examined. The following conclusions can be drawn:

- 438 1. Ring shear test revealed that (i) shear displacement to achieve the residual stage
439 with high shear rate is greater than that of the low shear rate; (ii) Both the peak
440 and residual friction coefficient became smaller with increase of shear rate for
441 each sample; (iii) The greater difference between the peak and the residual friction
442 coefficient in loess samples could be attributed to relatively well-developed
443 slickenside on the shear surface.
- 444 2. At the two shear rates, there was a nonlinearly decrease trend of the residual
445 friction coefficient with the normal stress in all loess samples. The difference
446 between the friction coefficients, $\tau_r/\sigma_n(1) - \tau_r/\sigma_n(0.1)$ was found to decrease
447 with normal stress in Ydg and Dbz specimens while increase with normal stress in



448 D_{rg} specimens, indicating that CF may be closely associated with shear rate effect
449 on residual friction coefficient with normal stress.

450 3. The difference at the two shear rates, $\phi_r(1) - \phi_r(0.1)$, under each normal stress
451 level were either negative or positive. However, under all normal stress, the
452 difference at the two shear rates $\phi_r(1) - \phi_r(0.1)$ was found to be negative. Such
453 negative shear rate effect on loess could be attributed to greater ability of clay
454 particles in specimen to restore broken bonds at low shear rates.

455 4. The relationships between the ϕ_r under two shear rates and soil properties (LL, I_p),
456 demonstrated that the ϕ_r at both shear rates decreased gradually with the
457 increasing of LL and I_p. However, no clear correlations between the difference in
458 the ϕ_r at low and high shear rates and the soil properties were found.

459

460



461 **Code availability:** Code can be made available by the authors upon request.

462 **Data availability:** Data can be made available by the authors upon request.

463 **Author contributions:** BL,JP and QH conceived and designed the method; BL
464 produced the results, and wrote the original manuscript under the supervision of JP.
465 JP and QH writing-review and editing.

466 **Competing interest:** The authors declare that they have no conflicts of interest.


467 **Acknowledgments:** This research was supported by the Major Program of National
468 Natural Science Foundation of China (Grant No. 41790440), the National Natural
469 Science Foundation of China (No.41902268) and the China Postdoctoral Science
470 Foundation (No. 2019T120871).



471 **References**

- 472 ASTM: (D422)Standard test method for particle-size analysis of soils. 2007.
- 473 Bhat, D. R.: Effect of shearing rate on residual strength of kaolin clay, PhD, Graduate school of Science
474 and Engineering, Ehime University, Japan, 2013.
- 475 Bishop, A. W.: Shear strength parameters for undisturbed and remoulded specimens., Foulis and Co,
476 3–58, 1971.
- 477 Bishop, A. W., Green, G. E., Garga, V. K., Andresen, A., and Brown, J. D.: A new ring shear apparatus
478 and its application to the measurement of residual strength, *Geotechnique*, 21, 273-328, 1971.
- 479 Bromhead, E.: The stability of slopes, blackie academic and professional, London. UK, 1992. 1992.
- 480 Chen, X. P. and Liu, D.: Residual strength of slip zone soils, *Landslides*, 11, 305-314, 2013.
- 481 Dijkstra, T., Rogers, C., Smalley, I., Derbyshire, E., Li, Y. J., and Meng, X. M.: The loess of north-central
482 China: geotechnical properties and their relation to slope stability, *Engineering Geology*, 36, 153-171,
483 1994.
- 484 Ding, H.: Ring shear tests on strength properties of loess in different regions. (In Chinese), Master,
485 Northwest A&F University, 2016.
- 486 Eid, H. T.: Stability charts for uniform slopes in soils with nonlinear failure envelopes, *Engineering*
487 *Geology*, 168, 38-45, 2014.
- 488 Fan, X., Xu, Q., Scaringi, G., Li, S., and Peng, D.: A chemo-mechanical insight into the failure mechanism
489 of frequently occurred landslides in the Loess Plateau, Gansu Province, China, *Engineering Geology*,
490 228, 337-347, 2017.
- 491 Gibo, S., Gassara, K., and Ohtsubo, M.: Residual strength of smectite-dominated soils from the
492 Kamenose landslide in Japan, *Can Geotech J*, 24, 456–462, 1987.
- 493 Gratchev Ivan, B. and Sassa, K.: Shear strength of clay at different shear rates, *Journal of Geotechnical*
494 *and Geoenvironmental Engineering*, 141, 2015.
- 495 Grelle, G. and Guadagno, F. M.: Shear mechanisms and viscoplastic effects during impulsive shearing,
496 *Géotechnique* 41, 60, 91–103, 2010.
- 497 Kimura, S., Nakamura, S., and Vithana, S. B.: Influence of effective normal stress in the measurement
498 of fully softened strength in different origin landslide soils, *Soil Till Res*, 145, 47-54, 2015.
- 499 Kimura, S., Nakamura, S., Vithana, S. B., and Sakai, K.: Shearing rate effect on residual strength of
500 landslide soils in the slow rate range, *Landslides*, 11, 969-979, 2014.
- 501 Kramer, S., Wang, C., and Byers, M.: Experimental measurement of the residual strength of particulate
502 materials, *Physics and mechanics of soil liquefaction*, 1999. 249-260, 1999.
- 503 Lemos, L.: Earthquake loading of shear surfaces in slopes, *Proc.11th I.C.S.M.F.E.*, 4, 1955-1958, 1985.
- 504 Leng, Y., Peng, J., Wang, Q., Meng, Z., and Huang, W.: A fluidized landslide occurred in the Loess
505 Plateau: A study on loess landslide in South Jingyang tableland, *Engineering Geology*, 236, 129-136,
506 2018.
- 507 Lupini, J. F., Skinner, A. E., and Vaughan, P. R.: The drained residual strength of cohesive soils,
508 *Geotechnique*, 31, 181-213, 1981.
- 509 Mesri, G. and Shahien, M.: Residual shear strength mobilized in first-time slope failures, *Journal of*
510 *Geotechnical and Geoenvironmental Engineering*, 129, 12-31, 2003.
- 511 Moeyersons, J., Van Den Eeckhaut, M., Nyssen, J., Gebreyohannes, T., Van de Wauw, J., Hofmeister, J.,
512 Poesen, J., Deckers, J., and Mitiku, H.: Mass movement mapping for geomorphological understanding
513 and sustainable development: Tigray, Ethiopia, *Catena*, 75, 45-54, 2008.



- 514 Morgenstern, N. R. and Hungr, O.: High Velocity ring shear tests on sand, *Geotechnique*, 34, 415-421,
515 1984.
- 516 Okada, Y., Sassa, K., and Fukuoka, H.: Excess pore pressure and grain crushing of sands by means of
517 undrained and naturally drained ring-shear tests, *Engineering Geology*, 75, 325-343, 2004.
- 518 Osipov, V., Nikolaeva, S., and Sokolov, V.: Microstructural changes associated with thixotropic
519 phenomena in clay soils, *Geotechnique*, 34, 293-303, 1984.
- 520 Perret, D., Locat, J., and Martignoni, P.: Thixotropic behavior during shear of a fine-grained mud from
521 Eastern Canada, *Engineering Geology*, 43, 31-44, 1996.
- 522 Picarelli, L.: Discussion on "A rapid loess flowslide triggered by irrigation in China" by D. Zhang, G.
523 Wang, C. Luo, J. Chen, and Y. Zhou, *Landslides*, 7, 203-205, 2010.
- 524 SAC: Standardization Administration of China (SAC), Ministry of Construction, Ministry of Water
525 Resources. In: China National Standards GB/T50123-1999: Standard for Soil Test Method, China
526 Planning Press, Beijing, 1999.
- 527 Sassa, K., Fukuoka, H., Wang, G., and Ishikawa, N.: Undrained dynamic-loading ring-shear apparatus
528 and its application to landslide dynamics, *Landslides*, 1, 7-19, 2004.
- 529 Shinohara, K. and Golman, B.: Dynamic shear properties of particle mixture by rotational shear test,
530 *Powder Technol*, 122, 255-258, 2002.
- 531 Skempton, A. W.: Long-term stability of clay slopes, *Geotechnique*, 14, 77-102, 1964.
- 532 Skempton, A. W.: Residual strength of clays in landslides, folded strata and the laboratory,
533 *Geotechnique*, 35, 3-18, 1985.
-  534 **Skepnton: Long-term stability of clay slopes, *Geotechnique*, 14, 77-102, 1964.**
- 535 Stark, T. D. and Vettel, J. J.: Bromhead ring shear test procedure, *Geotech Test J*, 15, 24-32, 1992.
- 536 Stark Timothy, D., Choi, H., and McCone, S.: Drained shear strength parameters for analysis of
537 landslides, *Journal of Geotechnical and Geoenvironmental Engineering*, 131, 575-588, 2005.
- 538 Summa, V., Margiotta, S., Medici, L., and Tateo, F.: Compositional characterization of fine sediments
539 and circulating waters of landslides in the southern Apennines–Italy, *Catena*, 171, 199-211, 2018.
- 540 Summa, V., Tateo, F., Giannossi, M., and Bonelli, C.: Influence of clay mineralogy on the stability of a
541 landslide in Plio-Pleistocene clay sediments near Grassano (Southern Italy), *Catena*, 80, 75-85, 2010.
- 542 Sun, P., Peng, J.-b., Chen, L.-w., Yin, Y.-p., and Wu, S.-r.: Weak tensile characteristics of loess in China —
543 An important reason for ground fissures, *Engineering Geology*, 108, 153-159, 2009.
- 544 Suzuki, M., Tsuzuki, S., and Yamamoto, T.: Residual strength characteristics of naturally and artificially
545 cemented clays in reversal direct box shear test, *Soils And Foundations*, 47, 1029-1044, 2007.
- 546 Terzaghi, K.: *Theoretical soil mechanics*, Chapman And Hall, Limited.; London, 1951.
- 547 Terzaghi, K., Peck, R. B., and Mesri, G.: *Soil mechanics in engineering practice*, John Wiley & Sons,
548 1996.
- 549 Tika, T.: Ring shear tests on a carbonate sandy silt, *Geotechnical Testing Journal*, 22, 1999.
- 550 Tika, T. E. and Hutchinson, J. N.: Ring shear tests on soil from the Vaiont landslide slip surface,
551 *Geotechnique*, 49, 59-74, 1999.
- 552 Tika, T. E., Vaughan, P. R., and Lemos, L. J. L. J.: Fast shearing of pre-existing shear zones in soil,
553 *Geotechnique*, 46, 197-233, 1996.
- 554 Tiwari, B.: Analysis of landslide mechanism of Okimi Landslide, M. Sc. Thesis, Niigata University, 2000.
555 2000.
- 556 Tiwari, B., Brandon, T. L., Marui, H., and Tuladhar, G. R.: Comparison of residual shear strengths from
557 back analysis and ring shear tests on undisturbed and remolded specimens, *Journal of Geotechnical*



- 558 and Geoenvironmental Engineering, 131, 1071-1079, 2005.
- 559 Tiwari, B. and Marui, H.: A new method for the correlation of residual shear strength of the soil with
560 mineralogical composition, Journal of Geotechnical and Geoenvironmental Engineering, 131,
561 1139-1150, 2005.
- 562 Vithana, S. B., Nakamura, S., Kimura, S., and Gibo, S.: Effects of overconsolidation ratios on the shear
563 strength of remoulded slip surface soils in ring shear, Engineering Geology, 131-132, 29-36, 2012.
- 564 Wang, J.-D., Li, P., Ma, Y., and Vanapalli, S. K.: Evolution of pore-size distribution of intact loess and
565 remolded loess due to consolidation, Journal of Soils and Sediments, 19, 1226-1238, 2019.
- 566 Wang, S., Wu, W., Xiang, W., and Liu, Q.: Shear behaviors of saturated loess in naturally drained
567 ring-shear tests. In: Recent Advances in Modeling Landslides and Debris Flows, Springer, 2015.
- 568 Wang, W.: Residual Strength of Remolded Loess in Ring Shear Tests., PhD Northwest A & F University
569 of China, 2014.
- 570 Wesley, L. D.: Residual strength of clays and correlations using atterberg limits, Geotechnique, 23,
571 669-672, 2003.
- 572 Zhang, D., Wang, G., Luo, C., Chen, J., and Zhou, Y.: A rapid loess flowslide triggered by irrigation in
573 China, Landslides, 6, 55-60, 2009.
- 574